Internal Pressure Fluctuations in Large Open Plan Buildings

M.T. Humphreys[1], J.D. Ginger[1] and D.J. Henderson[1]

[1]Cyclone Testing Station, College of Science and Engineering,
James Cook University, Townsville 4811, Queensland, Australia

Abstract

An internal pressure analysis was carried out on an open plan wind tunnel model for a range of nominally sealed (i.e. porous envelope) buildings, with and without dominant openings. The experimental results were compared to that obtained from analytical methods and also with design data specified in AS/NZS1170.2[10]. Increasing the level of porosity in a nominally sealed building resulted in an increase in internal pressure fluctuations, and mean and minimum internal pressures. However, increasing porosity with a dominant opening reduced internal pressure fluctuations, and mean, peak internal pressures. An analytical method used to determine the mean internal pressure in a nominally sealed building overestimated the measured mean pressure by 20%. AS/NZS1170.2[10] overestimated the minimum internal pressure in the nominally sealed building by 90% and slightly underestimated the maximum internal pressure. AS/NZS1170.2[10] also underestimated the maximum internal pressure in a building with a dominant opening by 20%, but overestimated the minimum internal pressure by 5%. The internal pressure fluctuations in nominally sealed buildings initially follow the external pressure fluctuations over the building, external frequencies above 7 to 17 Hz were attenuated, relating to a porosity discharge coefficient, k', in the range of 0.13 to 0.56. The relationship between the ratio of internal standard deviation pressure, and the external standard deviation pressure on a dominant opening, σ_{pI}/σ_{pE}, with the opening area to volume parameter, S*, were analysed and show good agreement with other studies. Dominant opening tests with an S* of 4.64, resulted in an increase in energy for internal pressure fluctuations at Helmholtz resonance frequency, of 36 Hz, resulting in an inertial coefficient, C_I, of 2.45.

Introduction

Industrial buildings are enclosed with steel cladding attached to portal frames and have a large open internal space. Large doors are installed to provide access to the interior space. The internal pressure fluctuations in a nominally sealed building (with a porous envelope) are generally small in magnitude compared to external pressures. However, these doors and windows may be susceptible to failure during windstorms, creating large openings which generate larger internal pressure fluctuations, increasing net loads and the vulnerability of the structural system. Hence internal pressures must be satisfactorily estimated in order to optimally design these types of buildings.

Internal pressure is generated by external pressure fluctuations on the building, is primarily dependent on the position and size of all openings in the envelope, the volume and the flexibility of the envelope. Flow through openings and the resultant internal pressure fluctuations will depend on the type of openings. Small openings such as gaps between the roof and walls and around doors and windows are considered as porosity (or background leakage) in an enclosed building, and defined as a nominally sealed case. A large opening created by the failure of a door or window will result in a dominant opening which usually is the critical design case.

This paper analyses the internal pressure fluctuations for a range of industrial building scenarios. The characteristics of pressure fluctuations are studied in nominally sealed buildings with and without a dominant opening, and peak internal pressures are compared with design data specified in AS/NZS1170.2 [10].

Analytical Methods

External and internal pressures, p_E, p_I, varying with time, t, can be presented as pressure coefficients, $C_p(t) = p(t)/(1/2\rho \bar{U}_h^2)$, where ρ is the density of air and $\bar{U}_h$ is the mean approach wind speed at mid-roof-height. Fluctuating pressures measured over an observation period are analysed statically to give $C_{\bar{p}}$, $C_{\sigma p}$, $C_{\hat{p}}$ and $C_{\check{p}}$ the mean, standard deviation, maximum and minimum pressure coefficients.

Nominally Sealed Case

Vickery [11] and Harris [3] analysed the nominally sealed case, and showed that internal pressure can be described by equation 1.

$$A_W k_W \sqrt{(C_{pE,W} - C_{pI})}$$
$$-A_L k_L \sqrt{(C_{pI} - C_{pE,L})} = \frac{V \bar{U}_h}{2 a_s^2} \frac{dC_{pI}}{dt} \qquad (1)$$

Where A is the accumulated open area over a surface, k is the discharge coefficient of the openings, V is the effective internal volume, a_s is the speed of sound and the subscripts I, E, W and L denote internal, external, windward and leeward surfaces respectively. For the same type of openings, $k_W = k_L$, and taking $dC_{pI}/dt = 0$, rearranging equation 1 gives equation 2. This gives relationship between the mean internal pressure and mean external pressure over the windward and leeward openings, and is used to define quasi-steady pressure coefficients, $C_{\bar{p}}$, given in AS/NZS1170.2 [10].

$$C_{\bar{p}I} = \frac{C_{\bar{p}E,W} \cdot A_W^2 + C_{\bar{p}E,L} \cdot A_L^2}{A_W^2 + A_L^2} \qquad (2)$$

Vickery [12] used a transfer function to describe how the external pressure fluctuations enter a nominally sealed building and defined a characteristic frequency, f_c, given in equation 3 above which the external pressures are attenuated and not passed into the building.

Here k' is the discharge coefficient for porous openings, which was found to be between 0.05 and 0.5 by Kim and Ginger [6].

$$f_c = \frac{1}{2\pi} \left(\frac{k' a_s^2 (A_W^2 + A_L^2)^{3/2}}{V \bar{U}_h A_W A_L \left(C_{\bar{p},W} - C_{\bar{p},L} \right)^{1/2}} \right) \qquad (3)$$

Dominant Opening Case

Holmes [4] analysed the internal pressures in a building with a single large opening in the envelope (i.e. the dominant opening case). He showed that the internal pressure fluctuations can be described by a Helmholtz resonator given by equation 4, where an 'air slug' oscillates back and forth through an opening to a volume. Here the first term describes the inertial energy, the second

damping, and the third background resistance. The forcing function is the external pressure at the opening, $C_{pE}(t)$.

$$\frac{C_I V}{a_s^2 \sqrt{A}} \ddot{C}_{pI} + \frac{1}{4k^2}\left(\frac{V \bar{U}_h}{a_s^2 A}\right)^2 \dot{C}_{pI}|\dot{C}_{pI}| + C_{pI} = C_{pE} \qquad (4)$$

$\dot{C}_{pI}$, $\ddot{C}_{pI}$ are the first and second time derivatives of $C_{pI}(t)$, A is the large opening area and C_I is an inertial coefficient, in the range of 0.7 to 2 for turbulent flow. Ginger et al. [2] showed that this equation can be re-arranged in terms of non-dimensional parameters, $S^* = A^{3/2}a_s^2/V\bar{U}_h^2$ and $\Phi_5 = \lambda_u/\sqrt{A}$, where λ_u is the integral length scale of turbulence. Also the ratio of internal to external pressure fluctuations can be described by a family of Φ_5 and S^* curves. The undamped resonant Helmholtz frequency of the system, $f_H = 1/2\pi \sqrt{a_s^2\sqrt{A}/C_I V}$.

The wind loading standard AS/NZS1170.2[10] specifies quasi-steady pressure coefficients, $C\bar{p}$, to determine peak design pressures, $\hat{p}$, in conjunction with the peak wind speeds, $\hat{U}$. The peak pressures measured, $C\hat{p}$, $C\check{p}$, are equivalent to $C\bar{p} \times G_u^2$. Where $G_u = \hat{U}/\bar{U} = 1.62$ is the velocity gust factor. and are rearranged to determine quasi-steady C_p values for comparison with AS/NZS1170.2[10].

Experimental Setup

A 400 mm wide × 200 mm long × 100 mm high building model with an additional volume under the turn-table to a depth of 600 mm, shown in figure 1, was tested in James Cook University's boundary layer wind tunnel. The tests were carried out in an open approach terrain equivalent to that of terrain category 2, as defined by AS/NZS1170.2[10], at a length scale of 1/200, with $\bar{U}_h \approx 10$ m/s.

Forty four external and four internal pressure taps were installed on the model. Tests were conducted for 16 seconds at approach wind direction, θ, in 10° intervals around the compass at a frequency of 625 Hz. Tests were repeated 5 times for each approach case.

The background leakage was modelled by installing 60 × 3 mm diameter and 175 × 1.5 mm diameter holes uniformly on the four walls, W1, W2, W3 and W4. Three large openings were also installed on the model which could be opened or sealed as needed on walls W1 and W4 of the model, illustrated in figure 1. Large openings, LO1 and LO2, are located on wall, W1, both have an area of 120 × 80 mm (9,600 mm²). Large opening, LO3, on wall, W4, is 40 × 80 mm (3,200 mm²).
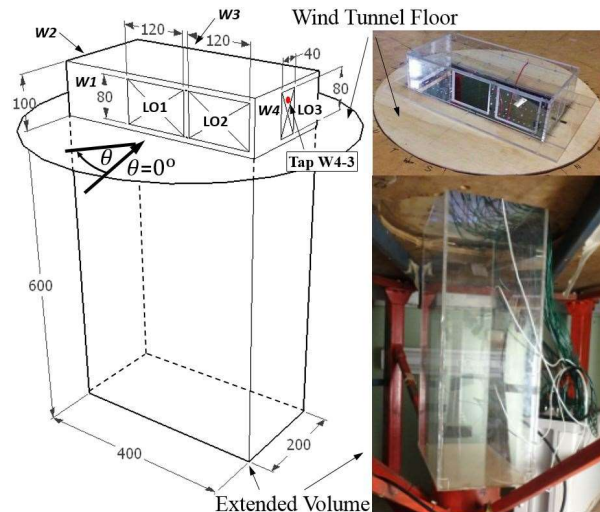

Figure 1. Wind tunnel model, all dimensions in millimetres

A range of test cases were conducted, shown in table 1, where each case shows large openings and porosity, ε, defined as percentage of open area to the wall surface area. For cases 7 and 8, the accumulated background leakage open area is equivalent to 5% and 10% of LO3 open area.

Case	Large Opening	Porosity, ε			
		W1	W2	W3	W4
1	-	0.61%	0.61%	0.61%	0.61%
2	-	0.35%	0.35%	0.35%	0.35%
3	-	0.26%	0.26%	0.26%	0.26%
4	LO1	0	0	0	0
5	LO2	0	0	0	0
6	LO3	0	0	0	0
7	LO3	0.30%	0.30%	0	0.30%
8	LO3	0.61%	0.61%	0	0.61%

Table 1. Wind tunnel model test cases

Results and Discussion

External Pressure Fluctuations

Figure 2 shows the external pressure spectra measured at a tap in the centre of the windward, leeward and side walls (W1, W3 and W4) for $\theta = 0°$. Figure 2 also shows the spectra for the spatially averaged pressure over the taps on LO1 and the spatially average pressure over the taps on all walls for $\theta = 0°$. Figure 2 shows the windward and side walls have the most energy in their fluctuations, with more energy in the tail of the side walls spectrum caused by the generation of a range of eddies by flow separation. The leeward wall is in the wake flow thus contains much less energy.

Figure 2 also shows that the spatial averaging of pressures over LO1 results in reduced fluctuations from around 10Hz. The instantaneous spatially averaged pressure over all the walls is the forcing function for the internal pressure in nominally sealed buildings. The spectral energy in the spatially averaged signal is much less than that on individual surfaces.
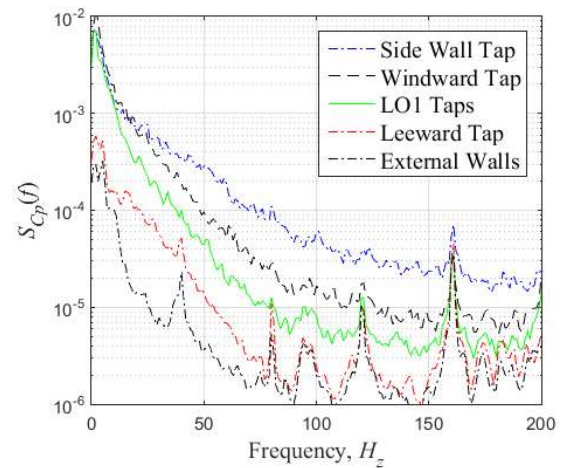

Figure 2. External pressure spectra on the windward, leeward and side walls, and spatially averaged pressures on LO1 and all walls, $\theta = 0°$

Internal Pressures – Nominally Sealed Case

Figure 3 gives the internal $C\bar{p}$ and internal maximum and minimum $C\bar{p}$ for Cases 1, 2 and 3 for $\theta = 0°$ to $90°$. Figure 3 shows Case 1 and 2 have similar mean and minimums for most directions, Case 3 has smaller pressures in all direction. AS/NZS1170.2[10] provides $C\bar{p}$ of -0.3 and 0. The internal maximum and minimum $C\bar{p}$ of +0.04 and -0.16 show AS/NZS1170.2[10] slightly overestimates the maximum, and is 90% more than the minimum.

From equation 2, the mean $C_{\bar{p}I}$ was determined to be $\approx$ -0.23 at θ = 0°, from the spatially averaged pressures on the windward and leeward surfaces, $C_{\bar{p}E,W}$ = +0.53, $C_{\bar{p}E,L}$ = -0.43, overestimating the minimum $C_{\bar{p}I}$ by 20%.
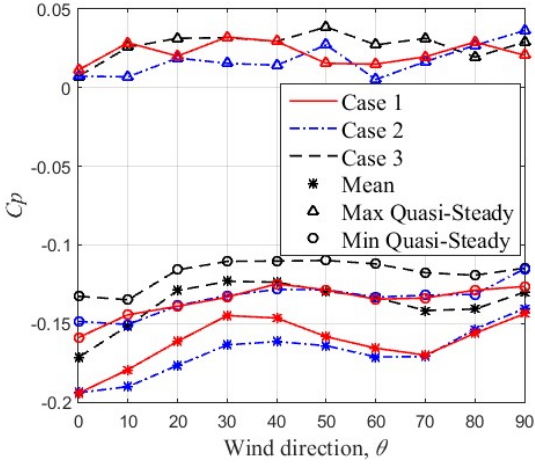

Figure 3. Mean and Quasi-Steady C_p – Cases 1, 2 and 3

Figure 4 shows the internal pressure spectra for Cases 1, 2 and 3 and external spectra of the spatially averaged pressure on all walls. Figure 4 shows as the magnitude of porosity increases, the magnitude of the internal fluctuations also increase. Figure 4 also shows the internal spectra initially follow the external pressure spectrum, with Case 3 diverging at 7 Hz and Cases 1 and 2 diverging between 7 and 17 Hz. Equation 3 shows that reducing the porosity, reduces f_c. Using the f_c values given from figure 4, equation 3 gives background leakage discharge coefficients in the range of 0.13 to 0.56. Sharma [8] showed that f_c is highly dependent on the magnitude of porosity and the approach turbulence intensity.
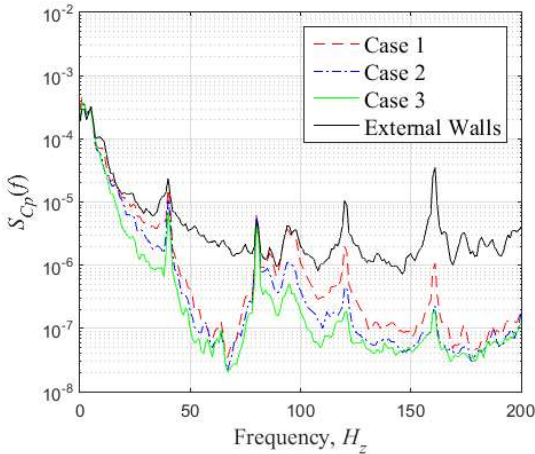

Figure 4. Internal pressure spectra – Cases 1, 2, 3 and external pressure spectrum averaged over all walls, $\theta = 0^o$

Internal Pressure – Large Opening Case

Figure 5 gives internal $C_{\bar{p}}$ and internal maximum and minimum $C_{\tilde{p}}$ for Cases 6, 7, 8, and external tap W4-3, for $\theta = 270^o$ to 90°. Figure 5 shows as background leakage increases, the internal $C_{\bar{p}}$ and internal maximum and minimum $C_{\tilde{p}}$ decrease. The maximum internal $C_{\tilde{p}}$ from Case 1 and 2 are slightly greater than the external tap, and similar to Case 8. The minimum $C_{\tilde{p}}$ is consistently lower than external tap W4-3.

AS/NZS1170.2[10] provides internal $C_{\tilde{p}}$ of +0.7 and -0.58 for LO3, and external $C_{\tilde{p}}$ of +1.05 and -0.86 for tap W4-3. The internal

maximum and minimum $C_{\tilde{p}}$ of +0.87 and -0.55 show AS/NZS1170.2[10] underestimated the maximum $C_{\tilde{p}}$ by 20%, and overestimated the minimum by 5%. Tap W4-3 external maximum and minimum $C_{\tilde{p}}$, +0.83 and -0.72 are about 80% of the standard.
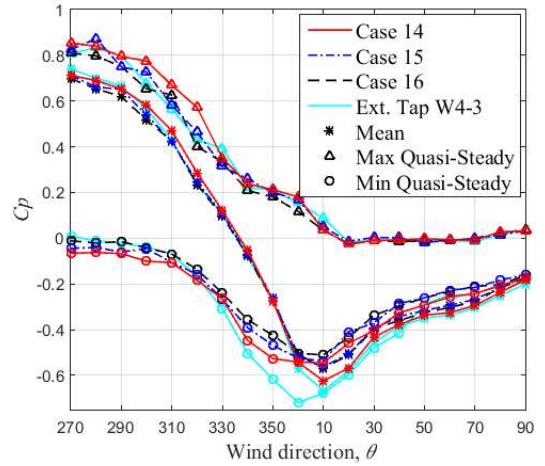

Figure 5. Mean and Quasi-Steady C_p – Cases 6, 7, 8 and External Pressure Tap W4-3

Figure 6 shows the internal pressure spectra for cases 6, 7 and 8, and the external pressure spectra of external tap W4-3 for $\theta = 270^o$. Figure 6 shows the internal spectra follow the external spectra until 22 Hz, where fluctuation increase towards the Helmholtz resonance frequency, f_H, of the system 36 Hz, and gives a C_I equal to 2.45, slightly higher than a typical value. Figure 6 also shows as the porosity increases, the fluctuations reduce and resonant peak is damped, reduced by 11% and 42% for Cases 7 and 8 respectively.
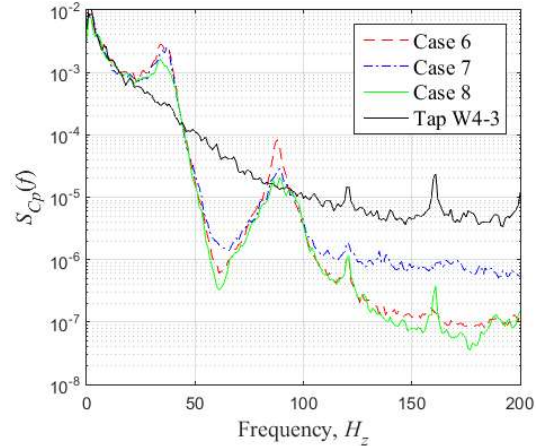

Figure 6. Internal pressure spectra – Cases 6, 7 and 8 and external pressure tap W4-3, $\theta = 270^o$

The ratio between the internal and external standard deviation can be expressed in terms of the opening area to volume parameter S^*. Figure 7 shows this relationship for Cases 4, 5 and 6. Figure 7 also has results from pervious wind tunnel tests by Ginger et al. [1], Holmes [4], Sharma and Richards [9] and Kopp et al. [7]. These studies were chosen as they have turbulence intensities around 20%, which is required for correct wind tunnel modelling of internal pressures.

The configurations tested have S^* values of 4.64 and 24.1, with standard deviation ratios ranging from 1.05 to 1.1. Holmes and Ginger [5] showed that this plot can be simplified and expressed theoretically by a bi-linear line. Here S^* values greater than 1, σ_{pI}/σ_{pE} = 1.1 and for $0.1 \leq S^* \leq 1.0$, σ_{pI}/σ_{pE} = 1.1 + 0.2$\log_{10}(S^*)$, matching the experimental data collected.
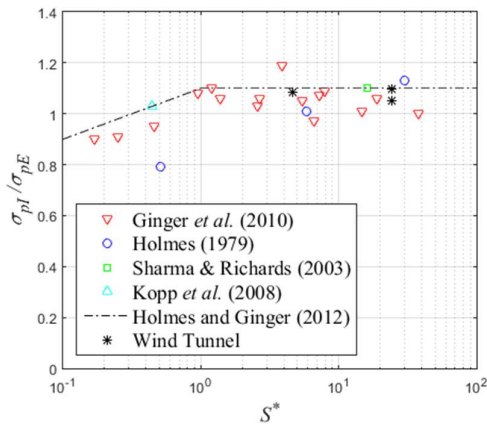
Figure 7. Ratio of internal to external pressure standard deviations vs S*

Conclusion

Internal pressures were analysed from conducting a series of wind tunnel model tests on a range of nominally sealed buildings with and without a dominant opening. The experimental results were compared to that obtained from analytical methods and also with design data specified in AS/NZS1170.2[10]. The following outcomes were reached:

- The mean and fluctuating internal C_ps were significantly lower than the external C_ps for nominally sealed buildings. Increasing the level of background leakage resulted in an increase in the internal $C\bar{p}$ and minimum $C\tilde{p}$.
- The internal pressure fluctuations for a building with a large opening follow the external fluctuation on the opening. Increasing the level of background leakage in a building with a large opening, resulted in a decrease in the internal $C\bar{p}$, and peak $C\tilde{p}$s, and damped fluctuations at Helmholtz frequency.
- Helmholtz resonance frequency for Cases 6, 7 and 8, of 36 Hz, results in a C_I equal to 2.45.
- The relationship between the ratio of the internal pressure standard deviation and external pressure standard deviation at a large opening, σ_{pI}/σ_{pE}, and the opening area to volume parameter, S*, matches previous studies.
- Internal pressure fluctuations in nominally sealed buildings initially follow the external pressure fluctuations over the building, external frequencies above 7 to 17 Hz were attenuated. These frequencies relates to a background leakage discharge coefficient, k', in the range of 0.13 to 0.56.
- The mean C_{pI} derived for the nominally sealed building from the summed spatially averaged mean C_{pE}s, overestimated the measured mean C_{pI} (-0.19), for $\theta = 0°$ by 20%.
- The minimum internal $C\tilde{p}$ from AS/NZS1170.2[10] for nominally sealed buildings (-0.3), was around 90% greater than the minimum $C\tilde{p}$ measured. The maximum internal $C\tilde{p}$ from AS/NZS1170.2[10] (0) was slightly less than that measured (+0.04).
- The maximum internal $C\tilde{p}$ measured for Cases 6 and 7 were slightly greater than the maximum external $C\tilde{p}$. For Case 8, the maximum $C\tilde{p}$ measured was similar to the maximum external $C\tilde{p}$ measured.
- The maximum internal $C\tilde{p}$ from AS/NZS1170.2[10] with a dominant opening (+0.7), underestimated the maximum internal $C\tilde{p}$ by 20% for LO3. AS/NZS1170.2[10] also overestimated the minimum internal $C\tilde{p}$ measured (-0.55) by 5%.

References

[1] Ginger, J.D., Holmes, J.D. & Kim, P.Y., Variation of internal pressure with varying sizes of dominant openings and volumes, *Journal of Structural Engineering,* vol. 136, pp. 1319-1326, 2010.

[2] Ginger, J.D., Holmes, J.D. & Kopp, G.A., Effect of building volume and opening size on fluctuating internal pressures, *Wind and Structures An International Journal,* vol. 11, pp. 361-376, 2008.

[3] Harris, R.I., The propagation of internal pressures in buildings, *Journal of Wind Engineering and Industrial Aerodynamics,* vol. 34, pp. 169-184, 7// 1990.

[4] Holmes, J.D., Mean and fluctuating internal pressures induced by wind, in *Fifth international conference on wind engineering*, Fort Collins, Collorado, U.S.A., 1979.

[5] Holmes, J.D. & Ginger, J.D., Internal pressures - The dominant windward opening case - A review, *Journal of Wind Engineering and Industrial Aerodynamics,* vol. 100, pp. 70-76, Jan 2012.

[6] Kim, P.Y. & Ginger, J.D., Internal pressures in buildings with a dominant opening and background porosity, *Wind and Structures An International Journal,* vol. 16, pp. 47-60, Jan 2013.

[7] Kopp, G.A., Oh, J.H. & Inculet, D.R., Wind-Induced Internal Pressures in Houses, *Journal of Structural Engineering,* vol. 134, pp. 1129-1138, 2008.

[8] Sharma, R.N., The influence of internal pressure on wind loading under tropical cyclone conditions, ResearchSpace@ Auckland, 1996.

[9] Sharma, R.N. & Richards, P.J., The influence of Helmholtz resonance on internal pressures in a low-rise building, *Journal of Wind Engineering and Industrial Aerodynamics,* vol. 91, pp. 807-828, 5// 2003.

[10] Standards Australia & Standards New Zealand, AS/NZS 1170.2:2011 (A4), in *Australian and New Zealand Standard Structural Design Part 2: Wind Actions*, ed: Standards Australia, Standards New Zealand, 2011.

[11] Vickery, B.J., Gust-Factors for Internal-Pressures in Low Rise Buildings, *Journal of Wind Engineering and Industrial Aerodynamics,* vol. 23, pp. 259-271, Jul 1986.

[12] Vickery, B.J., "Internal pressures and interactions with the building envelope," *Journal of Wind Engineering and Industrial Aerodynamics,* vol. 53, pp. 125-144, 11// 1994.